NICOLAUS COPERNICUS UNIVERSITY IN TORUŃ

Bulletin of Geography. Physical Geography Series, No. 24 (2023): 5–24
http://doi.org/10.12775/bgeo-2023-0001

Detection of flood-hazard-prone zones using GIS modeling and AHP method in urban areas: the case of Amman Governorate

Noah Al-Sababhah

Yarmouk University, Irbid, Department of Geography, Jordan
Correspondence e-mail: noah.h@yu.edu.jo
https://orcid.org/0000-0001-5969-6370

Abstract. The aim of this study is to creatively map areas at risk of urban flash flooding, which are generated in urban areas and are conditioned by the predisposition of the terrain and the degree of coverage and use in Amman, using the Analytic Hierarchy Process (AHP) Method and GIS Modeling. The AHP method involves the weighting of a number of factors adopted by comparison. The main factors considered in this study were elevation, slope, rainfall intensity, runoff, land use/land cover (LULC), flow accumulation, and measurement of stream power index (SPI); these were reclassified and weighted to map the levels of flood hazards in the study area. Each factor/criterion was weighted and assigned a rank or score using the Pairwise Comparison method to enable researchers to make a decision about the severity of the flood. The results show that about 28.2% of the study area has a high to very high risk of flooding and that flooding can be very strong in the north-western regions with high population density, while the risk becomes low in the eastern, south-eastern, and western arid and semi-arid regions with low population density.

Key words:
Flood Risk,
SPI,
GIS,
AHP,
SCS,
Amman Governorate

Introduction

Flood hazards are one of the environmental issues being studied nationally, regionally and globally (IPCC 2008). Floods are the most frequent hazards in arid and semi-arid regions, where flash floods are a hydrological process that causes excess surface water and flooding, taking into account that, at the present and in the future, this water can be a good source of water by water harvesting methods (Al-Qudah and Abu-Jaber 2009). In Jordan, floods are one of the main causes of damage to infrastructure and to public and private properties in urban areas. Most of the floods occur in the region as a result of sudden heavy rains due to atmospheric depressions in the winter months and atmospheric instability, which is a manifestation of weather disturbances that occur in the transitional seasons of spring and autumn (Greenbaun 2010; Nawaiseh and Sababhah 2017). Multi-criterion decision analysis (MCDA) is a method of decision-making using multiple factors inputs for decision-making processes. To explore a range of alternatives in terms of objective conflicts and multiple criteria, the MCDA technique is commonly used (Aher et al. 2013). Likewise, the AHP continues to be one of the most popular analytical techniques for complex decision-making problems and is widely used due to its flexibility and ease of use. An AHP method can be developed to have many levels to characterize a decision condition. The selected factors governing the suitability of the site are weighted using the AHP, which is aided by a pairwise comparison matrix that uses a scale of relative importance (Potter and Frevert 2010; Yasser et al. 2013; Al Raisi et al. 2014; Chaudhary et al. 2016; Al-Sababhah 2022). In fact, the AHP, introduced by Saaty (2008) is studied

extensively and used in applications where problems related to multiple criterion decision-making arise. The processing framework for evaluating and ranking the contribution of critical success factors is based on the successful implementation of a lean production technique with the help of the AHP approach (Ribeiro 1996; Aikhuele et al. 2014). A number of factors can be relied upon after classifying and weighting them using GIS, including rainfall, drainage basin area, slope, runoff, drainage density, soil texture, land use, communication lines, and infrastructure, with the aim of assessing flood risks and suggesting indicators of future risk. Based on the above, the AHP method integrated with GIS helps to determine the necessary measures to be taken before and after the occurrence of floods in order to locate the most likely affected areas and prevent flood occurrence (Kellens et al. 2008; Ozkan and Tarhan 2015; Al-sababhah 2018).

The current study aims to detect flood-hazard-prone zones in urban areas in Jordan based on integration between GIS and AHP methods, with the practical goal of creating a risk map that contributes to the planning and formulation of future plans and suggestions for engineering projects designed to limit the effects of flood risks.

In Jordan, as everywhere in the world, flood risk is linked to several physical-climatic and anthropogenic factors and poses several problems with socio-economic and environmental consequences; floods have consequences both in eroded zones upstream, where it could lead to desertification, and downstream in deposition zones where it can cause siltation of structures.

Materials and methodology

Study area

Amman, the capital of Jordan, is located in the north-western district of Jordan, geographically lies between 35°39'E and 37°13'E longitude and 31°14'N and 32°04'N latitude and covers an area of 7,582 km², representing 9% of the total area of Jordan. The study area can be subdivided into 22 population settlements, distributed geographically into nine main regions. The population is about 5.1 million people according to the latest census and estimates (Greater Amman Municipality statistics). The area includes many hills with valleys separating them, which may increase the risk of flooding to population and infrastructure. Amman Governorate is bordered by Zarqa Governorate to the north and north-east, Madaba and Balqa governorates to the west, and by the governorates of Karak and Ma'an to the south. It also reaches to the borders of Saudi Arabia into the south-east (Fig. 1a). Climatologically, the long-term analysis of temperature showed that the area's average temperature was ~17.8°C, with a mean annual minimum and maximum temperature between 16.1°C and 20°C, respectively (Fig. 1b). Also, the long-term analysis observed a regional rainfall average of 254 mm per year (i.e., from ~25 mm minimum in the south-east to 520 mm maximum in the north-west area) (Fig. 1c). Finally, the study area can be subdivided into three climatic regions, including arid, semi-arid and semi-humid regions (Fig. 1d). Amman is situated on the East Bank Plateau, an upland characterized by three major rivers that run through it. Originally, the city was built on seven hills, and the terrain is typified by their slopes. This increases the possibility of frequent flash floods, particularly in commercial activity sites and high population density areas. Furthermore, the difference in elevation and slope plays a major role in the prevailing environmental conditions.

Flood risk contributing factors

The intensity and frequency of occurrence of natural hazards as well as the increase in the world's population, and in particular the population density in areas affected by dangerous natural phenomena, result in interest in the development of the concept of susceptibility to such events. In the last two decades, there have been numerous attempts to quantify it, most often as an element of the risk assessment of losses. Literature reviews take up the challenge of tracking the development of vulnerability indicators, and the issue of vulnerability assessment is constantly in the study phase. In order to estimate the spatial distribution of flood risk areas, seven factors were used: Elevation, Slope (Degree), Rainfall Intensity (mm), Runoff (mm), LULC, Flow Accumulation (pixel) and SPI. The choice of these factors represents an attempt to obtain the highest accuracy for Flood-Hazard-Prone Zones by selecting as many factors as possible, shown as follows:

- ***Elevation***: The use of high-resolution DEMs is commonly used in flood risk modeling; it is also critical in creating highly accurate maps of

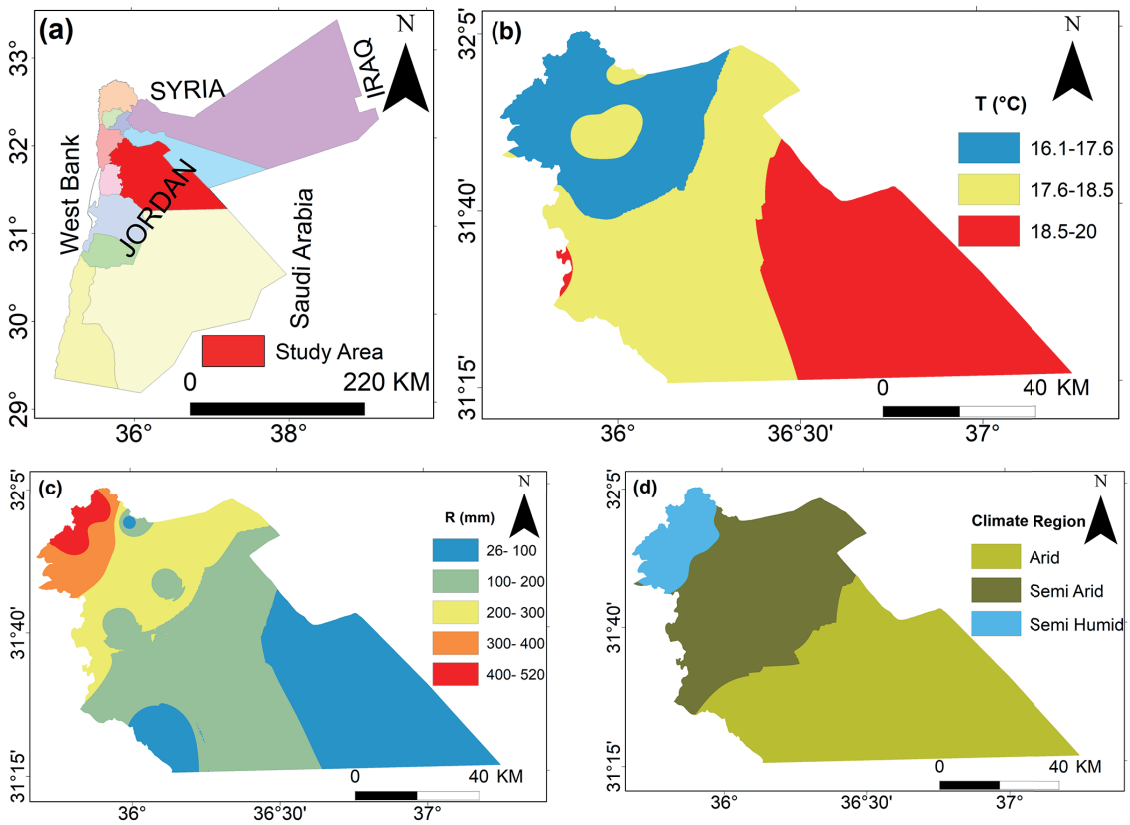

Fig. 1. (a) Study area location, (b) air temperature (°C), (c) rainfall (mm), (d) climate regions

flood risk hotspots. (Haile and Rientjes 2005; Puno and Amper 2016; Al-Sababhah 2023). The elevation ranges from -46 m (below sea level) to 1080 m (above sea level) in the study area (Fig. 2a).

- ***Slope***: The slope gradient is a crucial factor that affects flood risk from the land surface. The slope is one of the most important topographic features that cause flood risk (Andualem et al. 2020). The slope ranges from (0 to 55°) in the study area (Fig. 2b).
- ***Rainfall Intensity***: The effect of rainfall intensity characteristics as a major determining factor is crucial in order to deal with observed variability in flood risk, (Ran et al. 2012). The rainfall intensity ranges from 31 to 210 mm (Fig. 2c).
- ***Runoff:*** The close relationship between floods and rainfall is due to the impact on surface runoff in high-intensity storms that cause increased flow velocity, and higher runoff results in higher rates of flood risk (Falkland 1993). The runoff ranges from 1 mm to 133 mm in the study area (Fig. 2d).
- ***LULC:*** LULC are critical factors influencing surface runoff (Sinshaw et al. 2021). LULC changes were considered significant factors in floods in the study area – in particular, impermeable urban areas that increased the speed of runoff in combination with other factors. In this regard, seven types of LULC were recognized in the study area. Land-use/land cover classes were investigated and computed as presented in (Fig. 2e).
- ***Flow Accumulation***: Flow accumulation is a contributing factor in the occurrence of floods, defined as the cumulative flow downslope. Also, it is very beneficial for identifying flood hotspots. From a SPIll of bank-full discharge, a significant part of the low-lying area is flooded due to insufficiency in water outflow (Nie et al. 2011). The flow accumulation in the study area is shown in Figure 2f.
- ***SPI***: Flood events caused by water are directly linked to slope morphology in the areas. Assuming the flow is proportional to the catchment area and the pitch, the potential energy for runoff is also an indicator (Kakembo et al. 2009; Danielson 2013). The highest focus on flood risk has been the higher range of SPIs.

The SPI ranges from -13.8 to 13.2 in the study area (Fig. 2g).

Materials

The long-term (1980–2020) climatic data used in this assessment constitute the daily, monthly, and annual rates of rainfall for 19 climatic stations (Table 1).

Also, this work is based on two remote-sensing datasets obtained, namely (I) Landsat-8 surface reflectance data freely available from the United States Geological Survey (USGS [http://www.usgs.gov/]) during 2018–21; and (II) ASTER GDEM (https://asterweb.jpl.nasa.gov/gdem.asp) data freely available from NASA. As for the soil texture data, it was obtained from the soil survey records of the Jordanian Ministry of Agriculture for 1993–2021.

Methodology

In this paper, we use the Analytic Hierarchy Process (APH) and GIS Modeling to detect flood-hazard-prone zones in urban areas in Amman, the capital of Jordan. This AHP method consists of a weighting of a number of factors adopted by comparison, as well as a pair of factors that may control floods in this area. The main factors considered in this study were Elevation, Slope, Rainfall Intensity, Runoff, LULC, Flow Accumulation and SPI.

SCS-CN Method (USDA 2004)

The method that we selected for our study is the SCS-CN Method. In hydrological modeling, runoff estimation is one of the most important elements when analyzing flood risk. There is a number of empirical methods for its estimation. The most commonly and widely used empirical method is the Soil Conservation Service-Curve Number Method (SCS) developed by the United States Department of Agriculture and Soil Conservation Service (USDA-SCS) to estimate surface runoff. This method is very popular due to its simplicity, flexibility and requirement of a single parameter called Curve Number (CN) for the computation of runoff. Hydrologic soil group number, land use type and vegetation cover are the basic catchment characteristics used for curve number calculations. The equation for surface runoff is given in Eq. (I).

$$Q = \frac{(P-I_a)^2}{(P-I_a+S)} \quad \text{(I)}$$

Where, Q represents accumulated runoff or rainfall excess in mm, P is rainfall depth in mm, I_a is initial abstraction in mm, and S is potential maximum retention in mm. The I_a is quantified as in Eq. (II).

$$Ia = 0.2S \quad \text{(II)}$$

The term S is given by Eq. (III).

$$S = \frac{25400}{CN} - 254 \quad \text{(III)}$$

Where CN is curve number for study area conditions; some modifications were done and now I_a = 0.3S, and the equation for discharge can now be written as Eq. (IV).

$$Q = \frac{(P-0.3S)^2}{(P-0.7S)} \quad \text{(IV)}$$

Table 1. List of climatic stations used in this study

Elev. (m)	Long. (E)	Lat. (N)	Climate Station	Elev. (m)	Long. (E)	Lat. (N)	Climate station
700	35°57'	31°42'	Gizeh	912	35°47'	32°	Fohais
870	36°06'	31°49'	Mowaqqar	955	35°54'	31°58'	Abdali
850	36°01'	31°52'	Sahab	910	35°53'	31°56'	Zahran
840	35°55'	31°51'	Khraibet Sooq	775	35°59'	31°59'	Marka
700	36°02'	32°01'	Ruseifa	600	35°47'	31°33'	El-Waleh
550	37°04'	31°32'	Omari	790	36°03'	31°15'	Qetraneh
700	35°39'	31°44'	Madaba	1060	35°50'	32°01'	Swaileh
650	35°53'	32°06'	Ain Basha	995	35°54'	32°01'	Jubaiha
600	36°37'	31°43'	South Azraq	825	35°49'	31°56'	Wadi Sir
				740	36°04'	31°23'	Swaqah

Source: own elaboration

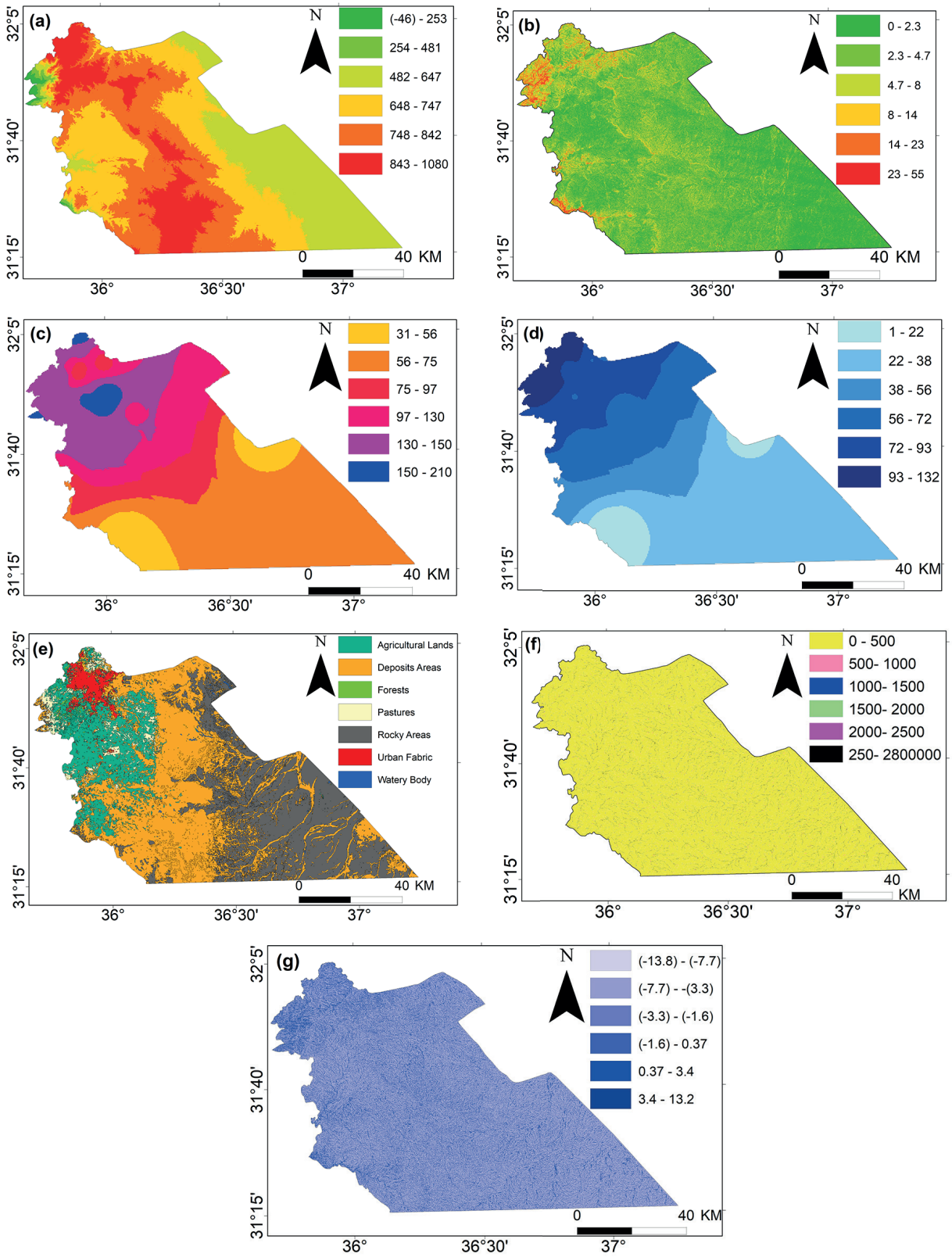

Fig. 2. Flood risk contributing factors: (a) elevation, (b) slope (degree), (c) rainfall intensity (mm), (d) runoff (mm), (e) LULC, (f) flow accumulation (pixel), (g) SPI

The curve numbers were adjusted; therefore, the total simulated runoff matched with the observed runoff data of the watersheds throughout the calibration process. The SCS-CNs were optimized according to the general condition of the land cover and landform within the study area. Table 2 indicates the rainfall-runoff values (mm) based on the SCS-CN method.

Measurement of SPI

The SPI index is one of the most important factors controlling land processes, since the erosive power of running water directly influences river cutting and slope toe erosion and flood (Nefeslioglu et al. 2008). The areas with high stream power indices have an excessive potential for flooding because they are representative of the potential energy procurable to entrain sediment (Kakembo et al. 2009). Assuming that discharge is associated with the specific catchment area, the erosive power of water flow can be measured by the SPI (Moore et al. 1991), as expressed in Eq. (V).

$$SPI = As \times tan\sigma \quad \text{(V)}$$

Where *As* represents the specific catchment area in meters and σ is the slope gradient in degrees. Also, Arc GIS can be used to measure SPI by Eq. (VI).

$$SPI = Ln((„Flow\ Accumulation" + 0.001) * * (("slope"/100) + 0.001)) \quad \text{(VI)}$$

For details, please refer to the website: https://www.wrc.umn.edu/randpe/agandwq/tsp/lidar.

Rainfall Intensity

In the study area, the maximum rainfall falling within a day recorded at the 19 stations representing the study area is used to determine rainfall intensity, as shown in Table 3.

The AHP Modeling Approaches

The AHP continues to be one of the most popular analytical techniques for complex decision-making problems and is widely used due to its flexibility and ease of use. An AHP can have many levels to characterize a decision condition. The selected factors governing the suitability of the site are weighted using the AHP, which is aided by a pairwise comparison matrix that uses a scale of relative importance (Yasser et al. 2013; Al Raisi et al. 2014; Chaudhary et al. 2016). This method consists of a weighting of the factors adopted by a comparison along with pairs of factors that may control flood in this area (Tairi et al. 2013). As mentioned above, the main factors considered in this study are Elevation, Slope, Rainfall Intensity, Runoff, LULC, Flow Accumulation and SPI. The AHP process may be subdivided into three steps: standardization, weight assignment and weighted linear combination.

Table 2. Values of rainfall-runoff (mm)

Runoff (mm)	Rainfall (mm)	Climate Station	Runoff (mm)	Rainfall (mm)	Climate Station
3.5	160	Gizeh	14.5	460	Fohais
4.2	170	Mowaqqar	11.7	390	Abdali
5.9	215	Sahab	8.8	300	Zahran
8.7	300	Khraibet Sooq	7.8	275	Marka
3.2	150	Ruseifa	5.9	220	El-Waleh
0.33	45	Omari	0.96	70	Qetraneh
9.6	300	Madaba	16.5	500	Swaileh
12.5	400	Ain Basha	17.4	320	Jubaiha
0.29	40	South Azraq	16.4	500	Wadi Sir
			0.96	65	Swaqah

Source: own elaboration

Citation: Bulletin of Geography. Physical Geography Series 2023, 24, http://doi.org/10.12775/bgeo-2023-0001

Table 3. Values of rainfall intensity (mm)

Avg	Maximum Rainfall (day)					Station	Avg	Maximum Rainfall (day)					Station
	5	4	3	2	1			5	4	3	2	1	
67.6	136	101	72	18	11	Gizeh	125.4	218	208	123	58	20	Fohais
60.02	110	92	66	20	12.1	Mowaqqar	85.2	190	91	85	33	27	Abdali
80.4	182	88	68	36	28	Sahab	74.6	170	80	75	27	21	Zahran
71.6	144	105	72	22	15	Khraibet Sooq	74.6	155	85	79	29	25	Marka
55.4	107	68	55	28	19	Ruseifa	53.4	100	70	60	22	15	El-Waleh
22.6	56	31	18	7	1	Omari	21.2	44	32	18	8	4	Qetraneh
88.8	185	95	78	48	38	Madaba	122.8	218	190	128	52	26	Swaileh
116.6	214	166	82	66	55	Ain Basha	126	210	200	133	62	25	Jubaiha
17	38	25	12	9	1	South Azraq	129.6	210	195	140	72	31	Wadi Sir
							33.8	81	44	37	6	1	Swaqah

Source: own elaboration

The MCDA mapping

There are different methods to determine the risk zones of flood, which calculate the amount of flood and which require a lot of data and criteria that can be applied to characterize the flood phenomenon in the study area. Among these qualitative methods, the MCDA is used to analyze a series of alternatives or objectives with a view to ranking them from most to least preferable using a structured approach. The end result of MCDA is often a set of weights linked to the various alternatives. The weights indicate the preference of the alternatives relative to each other. They may also be seen as the received advantage or disadvantage when changing from one alternative to another. The choice of methodologies for the calculation of these weights varies from text to text. Several authors (Stewart and Scott 1995; Joubert et al. 1997; Ayalew and Yamagishi 2005; Kourgialas and Karatzas 2011) have used the methods highlighted by Malczewski (1999) when calculating weights in MCDA. The AHP developed by Saaty (1977, 1984), is the simplest of the multi-criterion methods. It is based on the synthesis and aggregation of weights assigned to the criteria of the different levels of the hierarchy. The weights and ranks of each parameter were assigned after the pair-wise comparison using the rating scale (Table 4).

Pair-wise comparison matrix

Pairwise comparison of the approved factors in the application of the AHP requires the development of a pairwise comparison matrix between the seven factors affecting flood, and this depends on the importance of each factor in the occurrence of flood. These factors are Elevation, Slope, Rainfall Intensity, Runoff, LULC, Flow Accumulation and SPI, where the pairwise comparison of each pair of elements in each level is compared with respect to the corresponding elements in the level above them. This is done in terms of their importance. The comparisons can then be represented by multiple square matrices (Chen 2006) as Eq. (VII).

$$C = (Cij)nxn \quad \text{(VII)}$$

Where *C* is consistency ratio, with each matrix of order n as the matrix (Table 5), in order to make a decision.

The representation of matrices that have reciprocal properties (Saaty 1980) is done by Eq. (VIII).

$$C = (1/Cij)nxn \quad \text{(VIII)}$$

After the pairwise comparisons have been completed, a weight value is assigned to the element that has a higher importance in the pair. As for the less important element in the pair, a reciprocal value will be assigned to it. Normalization followed by the averaging of the weights is then done to obtain the relative weight for each of the elements in the hierarchical model. Let's get to the matrix. See (Table 6).

Then, the pairwise comparison matrix will be normalized by Eq. (IX).

$$C = (Cij)nxn \quad \text{(IX)}$$

Where each element in the matrix will be divided by the sum of its columns (Bunruamkaew

Table 4. Scale of comparisons of criteria (Saaty 1984)

Important	Verbal definition of the importance of one factor over the other	Scale
More Important	Extremely	9
	Very strongly	7
	Strongly	5
	Moderately	3
	Equally important	1
Equally Important	Moderately	1/3
	Strongly	1/5
	Very Strongly	1/7
Less Important	Extremely	1/9

Source: own elaboration

and Murayama 2011) to get the following matrix (Table 7).

Weights of all factors in the hierarchical model are based on the researcher's vision, and by referring to previous studies within the same field, pair-wise comparisons and ranking of factors were done (Table 8). In analyzing flood risk areas, slope was considered the most influential factor (highly sensitive to flood), whereas SPI was considered the least sensitive to flooding risk. The values in each cell represent the scale of relative importance for the given paired factors. The diagonal has a value of "1" throughout because the diagonal represents factors being compared to itself with the scale of "1" (equal importance). On the lower diagonal, the values of the scale are infractions because the factors are being paired in the reverse order and the scale of relative importance is given as the reciprocal of the upper diagonal pair-wise comparisons (Andualem et al. 2020). Hence, for identifying the flooding hotspot areas in Amman, factors are ranked as follows: elevation first, slope second, rainfall third, runoff fourth, LULC fifth, flow accumulation sixth and SPI seventh.

These verbal judgments are based on a good expert knowledge of the field and the importance of each factor in the phenomenon of flood. To calculate the weights of each factor, we will need to convert each value in the table of the comparison matrix in Table 8 to a percentage of the sum per column. Then the weight of each factor is the average of each row of the standardized matrix (Table 9).

Consistency analysis

In the AHP, the pair-wise comparisons in a judgment matrix are considered to be adequately consistent if the corresponding consistency ratio (CR) is less than 10% (Saaty 1980). First, the consistency index (CI) needs to be estimated. This is done by adding the columns in the judgment matrix and multiplying the resulting vector by the vector of priorities (i.e., the approximated eigenvector) obtained earlier. This yields an approximation of the maximum Eigenvalue, denoted by λmax. Table 10 refers to the

Table 5. Multiple Square Matrix

Factors	Elevation	Slope	Rainfall Intensity	Runoff	LULC	Flow Accumulation	SPI
Elevation	C11	C12	C13	C14	C15	C16	C17
Slope	C21	C22	C23	C24	C25	C26	C27
Rainfall Intensity	C31	C32	C33	C34	35	C36	C37
Runoff	C41	C42	C43	C44	C45	C46	C47
LULC	C51	C52	C53	C54	C55	C56	C57
Flow Accumulation	C61	C62	C63	C64	C65	C66	C567
SPI	C71	C72	C73	C74	C75	C67	C77

Source: own elaboration

Citation: Bulletin of Geography. Physical Geography Series 2023, 24, http://doi.org/10.12775/bgeo-2023-0001

Table 6. Representation of matrices that have reciprocal properties

Factors	Elevation	Slope	Soil Txt	Rainfall	LULC	Flow Accumulation	SPI
Elevation	1/C11	1/C12	1/C13	1/C14	1/C15	1/C16	1/C17
Slope	1/C21	1/C22	1/C23	1/C24	1/C25	1/C26	1/C27
Rainfall Intensity	1/C31	1/C32	1/C33	1/C34	1/C35	1/C36	1/C37
Runoff	1/C41	1/C42	1/C43	1/C44	1/C45	1/C46	1/C47
LULC	1/C51	1/C52	1/C53	1/C54	1/C55	1/C56	1/C57
Flow Accumulation	1/C61	1/C62	1/C63	1/C64	1/C65	1/C66	1/C567
SPI	1/C71	1/C72	1/C73	1/C74	1/C75	1/C67	1/C77

Source: own elaboration

Table 7. Decision matrix

Factors	Elevation	Slope	Rainfall Intensity	Runoff	LULC	Flow Accumulation	SPI
Elevation	C10/10	C10/8	C10/7	C10/5	C10/3.33	C10/2	C10/1
Slope	C8/10	C8/8	C8/7	C8/5	C8/3	C8/2	C8/1
Rainfall Intensity	C7/10	C7/8	C7/7	C7/5	C7/3	C7/2	C7/1
Runoff	C5/10	C5/8	C5/7	C5/5	C5/3	C5/2	C5/1
LULC	C3/10	C3/8	C3/7	C3/5	C3/3	C3/2	C3/1
Flow Accumulation	C2/10	C2/8	C2/7	C2/5	C2/3	C2/2	C2/1
SPI	C1/10	C1/8	C1/7	C1/5	C1/3	C1/2	C1/1

Source: own elaboration

consistency matrix used to calculate the consistency ratio.

Then, the CI value is calculated using Eq. (X).

$$CI = (\lambda max - n)/(n - 1) \quad \text{(X)}$$

Where λmax is calculated using Eq. (XI).

$$\lambda max = \sum_{i=0}^{n} (Xij) \times (Wij) \quad \text{(XI)}$$

Next, the consistency ratio CR is calculated by using Eq. (XII).

$$CR = (CI/RI) \times 100 \quad \text{(XII)}$$

Where *RI* refers to the mean of an Index of Consistency; the matrix Order and *CI* refer to the Index of Consistency as expressed. A randomly generated pairwise comparison matrix is used

Table 8. Comparison matrix of the seven factors adopted

Factors	Elevation	Slope	Rainfall Intensity	Runoff	LULC	Flow Accumulation	SPI	Sum	Weight (%)
Elevation	1.00	1.25	1.43	2.00	3.33	5.00	10	24.01	28.09
Slope	0.80	1.00	1.60	1.14	1.60	4.00	8	18.14	21.22
Rainfall Intensity	0.70	0.88	1.00	1.40	2.33	3.50	7	16.81	19.66
Runoff	0.50	0.63	0.71	1.00	1.67	2.50	5	12.01	14.04
LULC	0.30	0.38	0.43	0.60	1.00	1.50	3	7.20	8.43
Flow Accumulation	0.20	0.25	0.40	0.40	0.67	1.00	2	4.92	6.00
SPI	0.10	0.13	0.14	0.20	0.33	0.50	1	2.40	2.81
Sum	3.60	4.50	5.71	6.74	10.93	18	36	85.49	100

Source: own elaboration

Table 9. Standardized matrix of flood factors

Factors	Elevation	Slope	Rainfall Intensity	Runoff	LULC	Flow Accumulation	SPI	Sum	Avg	Weight %
Elevation	0.28	0.28	0.25	0.30	0.30	0.28	0.28	1.96	0.28	28.04
Slope	0.22	0.22	0.28	0.17	0.15	0.22	0.22	1.48	0.21	21.21
Rainfall Intensity	0.19	0.19	0.18	0.21	0.21	0.19	0.19	1.37	0.20	19.63
Runoff	0.14	0.14	0.13	0.15	0.15	0.14	0.14	0.98	0.14	14.02
LULC	0.08	0.08	0.08	0.09	0.09	0.08	0.08	0.59	0.08	8.41
Flow Accumulation	0.06	0.06	0.07	0.06	0.06	0.06	0.06	0.41	0.06	5.89
SPI	0.03	0.03	0.03	0.03	0.03	0.03	0.03	0.20	0.03	2.80
Sum	1	1	1	1	1	1	1	7	1	100

Source: own elaboration

to obtain the random consistency index, *RI*. The values of RI for matrices of order are 1 to 15 (1 to 10 elements in one level) (Table 11) (Saaty T. 1984; Saaty R. 2016). The RI value in this study was 1.32.

If λ max is the most massive value of the matrix of its own, the matrix can be determined easily; 'n' is the matrix sequence. The CR is a ratio of the random index to the matrix consistency index, the value of which is from 0 to 1. A CR of 0.1 or less is considered a respectable level, and over 0.1 implies a revision required because the individual factor ratings are not being handled uniformly (Malczewski 1999). When these approximations are applied to the previous judgment matrix, it can be verified that the following are derived: λmax= 7.02; CI = 0.0034 and CR = 0.0025.

Once the weighting is done, the different factors are adopted, and the coherence ratio value is acceptable. CR = 0.01, and the superposition of the seven input factors adopted will be carried out under ArcGIS software 10.4.1 according to Eq. (XIII).

$$Risk\ of\ Flood = (0.2809 * Elevation) + (0.2122 * Slope) + \\ + (0.1966 * Intensity\ of\ Rainfall) + (0.1404 * Runoff) + \\ + (0.843 * Land\ Use, Land\ Cover) + \\ + (0.06 * Flow\ Accumulation) + (0.0281 * SPI)$$

Processing of input data and interpolation methods

The spatial data were stored in a vector data format shape file by GIS 10.4.1 software, for spatial data administration and analysis, based on the database including spatial data of sites. Also, the spline interpolation approach in GIS was chosen since studies involving a small number of instances are best suited for it (Hutchinson 1998). The spline method is defined as a system of lower-degree polynomials that follow each other at the points of the input point field at various intervals (Malczewski 2006).

Results and discussion

The factors of flood risk are compared with each other by developing a comparison matrix. They are compared as the importance of one with respect to another and accordingly given a rating as per Saaty's scale. The present study was conducted to determine the zones of Amman Governorate in Jordan that have had frequent urban floods in recent years.

Reclassification of flood risk contributing factors

The model applied in this study allows for the determination of the zones sensitive to flooding in the study area. Based on the sensitivity classes of the factors that control flood risk, we have established

Table 10. Consistency measurement matrix

Factors	Weight %	Consistency measure	Acceptance
Elevation	28.04	0.0099	Accepted
Slope	21.21	0.0104	Accepted
Rainfall Intensity	19.63	0.0099	Accepted
Runoff	14.02	0.0099	Accepted
LULC	8.41	0.0099	Accepted
Flow Accumulation	5.89	0.0101	Accepted
SPI	2.80	0.0099	Accepted
Sum	100	0.0699	Accepted
CI=0.003 RI = 1.32 CR=0.002			

Source: own elaboration

Table 11. Random indices for matrices of comparisons (Saaty 1984)

Size	1	2	3	4	5	6	7	8	9	10
RI	0	0	0.58	0.9	1.11	1.24	1.32	1.41	1.45	1.49

the reclassification maps of the risk of flood in Amman, as follows:

- ***Elevation***: The DEMs map was reclassified into five major elevation classes depending on susceptibility to flooding. The higher the altitude of the area, the greater the possibility of having recurring floods as a result of high amounts of rain and vice versa (Fig. 3a).
- ***Slope***: The slope map was reclassified into five major slope classes depending on the Food and Agriculture Organization (FAO) slope classification and susceptibility to flooding. Areas that are found on flat and gentle slopes were taken as having very low and low susceptibility to flooding, and vice versa (Fig. 3b).
- ***Rainfall Intensity***: The most frequent floods occur in the areas with the highest rainfall intensity, and higher runoff causes higher rates of flood risk. On this basis, the rainfall intensity map was classified (Fig. 3c).
- ***Runoff:*** The most frequent floods occur in the areas with the highest surface runoff, and higher runoff causes higher rates of flood risk. On this basis, the runoff map was classified (Fig. 3d).
- ***LULC***: As mentioned above, impermeable urban areas and rocky areas have a very high probability of flooding, while agricultural and forest areas have a lower probability of flooding. On this basis, the LULC map was classified (Fig. 3e).
- ***Flow Accumulation:*** In the classified map, the higher the flow accumulation values, the higher the probability of flooding, due to the continuous accumulation of rainwater (Fig. 3f).
- ***SPI:*** Flood events are directly linked to slope morphology in the areas. The higher the SPI values, the higher the probability of flooding (Fig. 3g).

Weighting of flood risk contributing factors

The weighing process in multi-criterion models is subject to the researcher's decision as there are different methods available to determine weights, but these weights must be credible. All flooding contributing factors were classified into five categories that represent the degree of risk scale of that category on the possibility of flooding within the same factor. A standard scale of 1–9 according to the Sa'aty (1984) system was used to determine the degree of impact, with a value of 9 indicating a higher degree of risk. Referring to the above, these verbal judgments are based on a good expert knowledge of the field and of the importance of each factor in flooding. To calculate the weights of each factor, we will need to convert each value of the comparison matrix in Table 6 to a percentage of the sum per column in Table 7. Then, the weight of each factor is the average of each row of the standardized matrix. Table 12 indicates the weights

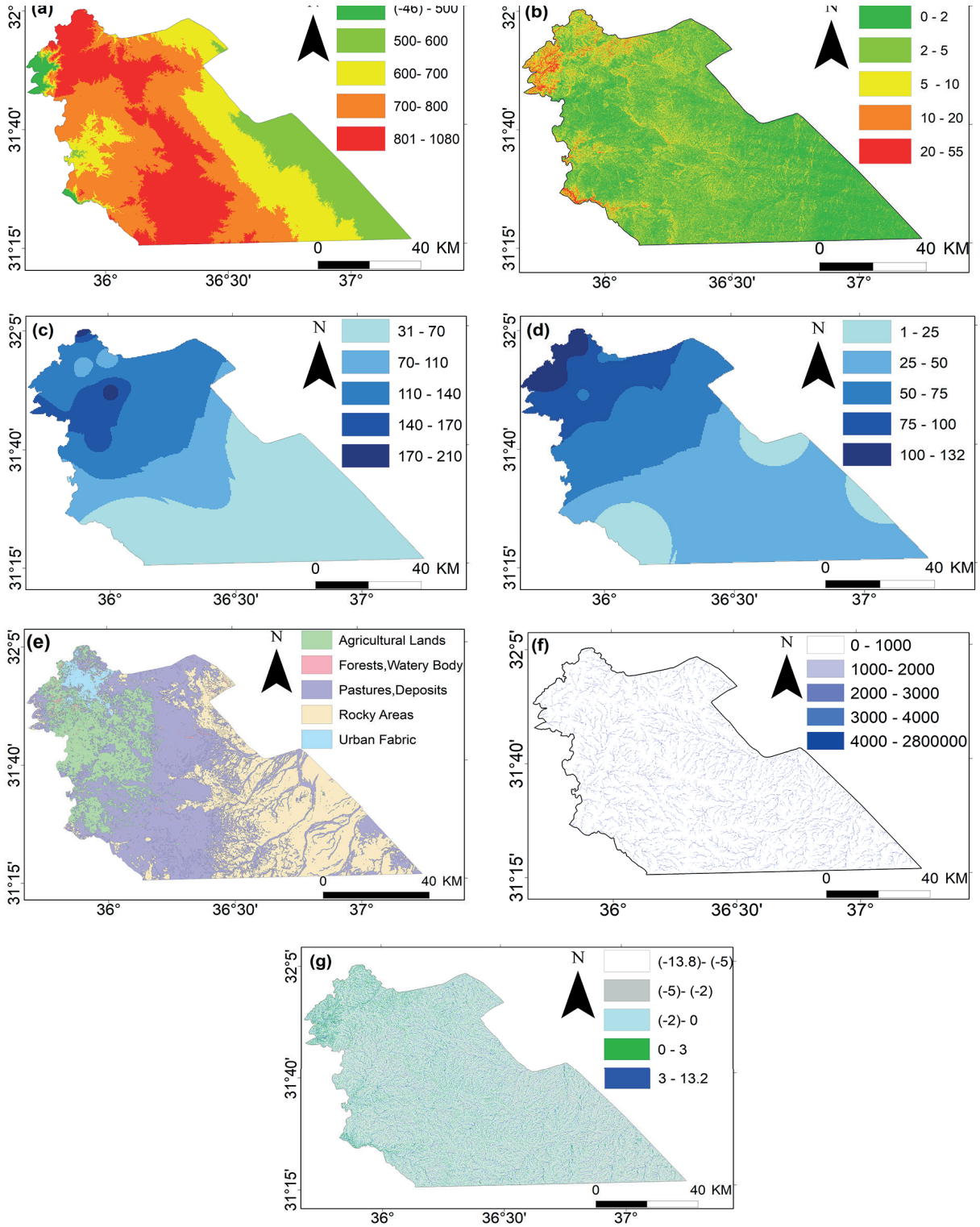

Fig. 3. Classified flood risk contributing factors: (a) elevation, (b) slope (degree), (c) rainfall intensity (mm), (d) runoff (mm), (e) LULC, (f) flow accumulation (pixel), (g) SPI

Citation: Bulletin of Geography. Physical Geography Series 2023, 24, http://doi.org/10.12775/bgeo-2023-0001

Table 12. Classification and weighting of factors

Percentage (%)	Total Weight	Weighting Rate	Proposed Weight	Risk Level	Domain	Factor
28	24.01	0.139	9	Very high	800–1084	Elevation
		0.054	7	High	700–800	
		0.039	5	Moderate	600–700	
		0.023	3	Low	500–600	
		0.023	1	Very low	(-46)–500	
21	18.14	0.111	9	Very high	0–2	Slope
		0.043	7	High	2–5	
		0.031	5	Moderate	5–10	
		0.019	3	Low	10–20	
		0.019	1	Very low	20–55	
18	16.81	0.088	9	Very high	170–210	Rainfall Intensity
		0.034	7	High	140–170	
		0.024	5	Moderate	110–140	
		0.015	3	Low	71–110	
		0.015	1	Very low	31–70	
15	12.01	0.074	9	Very high	100–132	Runoff
		0.029	7	High	75–100	
		0.021	5	Moderate	50–75	
		0.012	3	Low	25–50	
		0.012	1	Very low	1–25	
9	7.20	0.046	9	Very high	Rocky Areas	LULC
		0.018	7	High	Urban Fabric	
		0.013	5	Moderate	Pastures, Deposits Areas	
		0.008	3	Low	Agricultural Lands	
		0.008	1	Very low	Forests, Water Body	
6	4.92	0.028	9	Very high	2,800,000–4000	Flow Accumulation
		0.011	7	High	4000–3000	
		0.008	5	Moderate	3000–2000	
		0.005	3	Low	2000–1000	
		0.005	1	Very low	1000–0	
3	2.40	0.014	9	Very high	3–13.2	SPI
		0.005	7	High	0–3	
		0.004	5	Moderate	(-2)–0	
		0.002	3	Low	(-5)–(-2)	
		0.002	1	Very low	(-13.8)–(-5)	
100 %	85.49	1	Total			

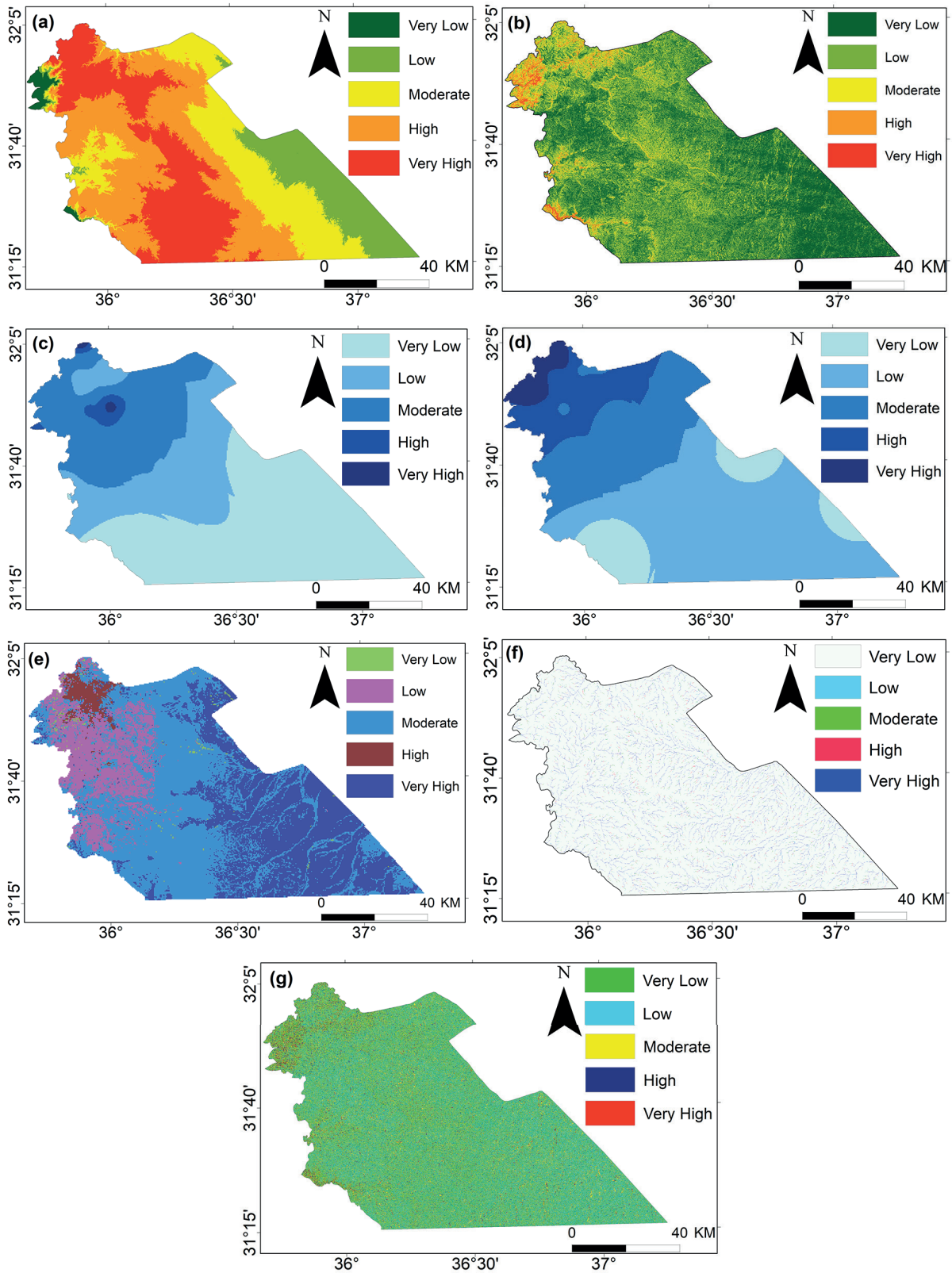

Fig. 4. Risk levels for flood risk contributing factors: (a) elevation, (b) slope (degree), (c) rainfall intensity (mm), (d) runoff (mm), (e) LULC, (f) flow accumulation (pixel), (g) SPI

Citation: Bulletin of Geography. Physical Geography Series 2023, 24, http://doi.org/10.12775/bgeo-2023-0001

Table 13. Distribution of risk levels for flooding contributing factors

Percentage (%)	Area (km²)	Risk Level	Domain	Factor
26.4	2000	Very high	800–1084	Elevation
34.1	2582.8	High	700–800	
23.8	1805	Moderate	600–700	
14.5	1101	Low	500–600	
1.2	93.2	Very low	(-46)–500	
100	7582		Total	
0.6	37.2	Very high	0–2	Slope
3.6	236	High	2–5	
14.5	957	Moderate	5–10	
32.3	2125.8	Low	10–20	
49.0	3226	Very low	20–55	
100	6582		Total	
0.3	19.5	Very high	170–210	Rainfall Intensity
1.8	135	High	140–170	
25.3	1921	Moderate	110–140	
24.3	1843	Low	71–110	
48.3	3663.5	Very low	31–70	
100	7582		Total	
3.3	250	Very high	100–132	Runoff
12.1	919	High	75–100	
24.2	1838	Moderate	50–75	
49.3	3740	Low	25–50	
11.0	835	Very low	1–25	
100	7582		Total	
33.7	2555	Very high	Rocky Areas	LULC
2.5	192	High	Urban Fabric	
48.0	3639	Moderate	Pastures, Deposits Areas	
15.3	1158	Low	Agricultural Lands	
0.5	38	Very low	Forests, Water Body	
100	7582		Total	

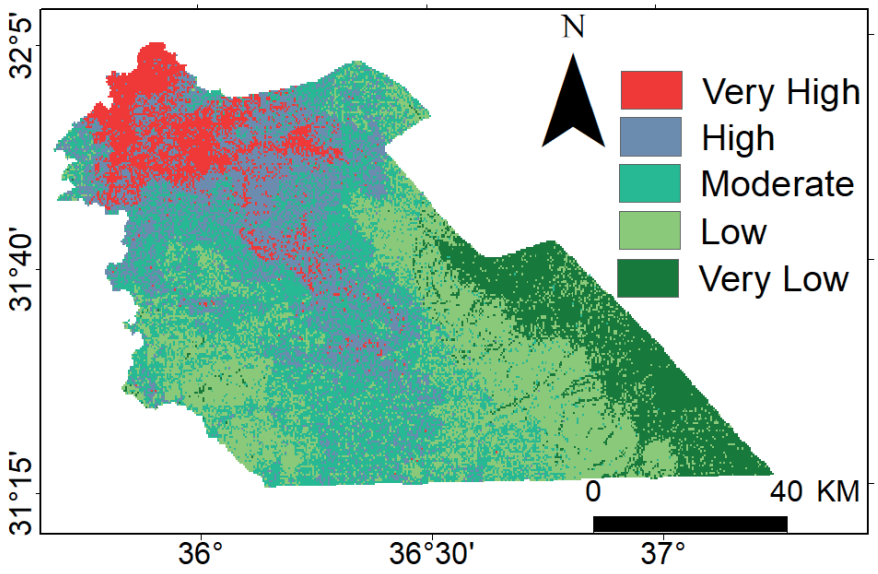

Fig. 5. Final flood risk map for the study area

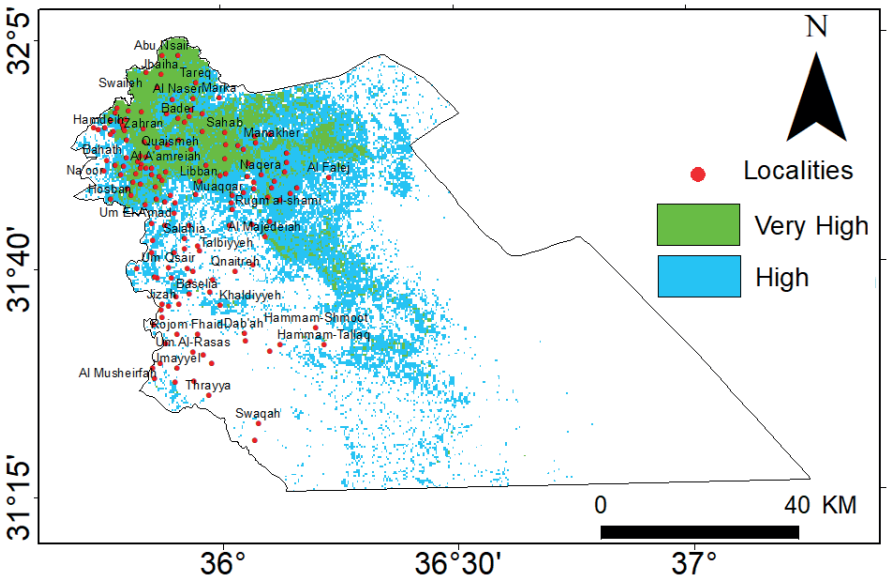

Fig.6. Distribution of flood risk areas according to population settlements in Amman

Table 14. Distribution of risk levels for flood risk

Risk level	Area (km²)	percentage (%)
Very High	635	8.4
High	1498	19.8
Moderate	2288	30.2
Low	2061	27.2
very Low	1100	14.5
Sum	7582	100

of the factors, the percentage of weights for each factor, the levels of flood risk, and the classification of factors.

The risk classes were assigned to the seven selected factors. Then the AHP pair-wise comparison matrix was constructed based on the preferences of each factor relative to the others. As input it takes pair-wise comparisons of the factors and it produces their relative weights as output. All flooding contributing factors were classified into five categories that represent the degree of risk scale of that category on the possibility of flood risk.

Risk levels for flooding contributing factors

Flood risk areas are classified into five risk levels according to the severity of flood. The spatial distribution of each class of flooding in percent was developed by the AHP method (Fig. 4).

Depending on the areas of the flood risk levels, the areas with a high or very high level of risk are about 50.5% for areas whose height is more than 700 m above sea level (Fig. 4a, Table 13). Areas that are found on flat and gentle slopes of less than 5 degrees were considered as having very high and high susceptibility to flooding (Fig. 4b, Table 13). As for Rainfall Intensity, areas with high or very high risk levels of flooding were about 2.1% of the total area (Fig. 4c, Table 13). Meanwhile, high and very high levels of risk for runoff represented about 15.4% of the total area (Fig. 4d, Table 13). Areas that are found in rocky areas and urban fabric were taken as having high and very high susceptibility to flooding. Their area constituted a percentage of 36.2% (Fig. 4e, Table 13). As for the levels of risk according to Flow Accumulation, its impact on floods was low within the built-up areas, according to the characteristics of the prevailing impermeable surface and sewage system. As for the areas with a very high risk, they represented about 1.2% of the total area (Fig. 4f, Table 13). Finally, areas with high SPI values were considered highly susceptible to flooding, whereas areas with low SPI values were classified as having low susceptibility to flooding. As can be seen from the spatial distribution of SPI, 8.1 % and 2.1 % of the area have been found to have a high and very high susceptibility to flooding (Fig. 4g, Table 13).

The use of GIS is considered one of the effective tools in determining flood risk areas as a multidimensional natural hazard, as it has a spatial dimension (Zerger 2002). In addition, it is important in supporting the spatial decision through building multi-criterion models to determine the areas of flood risk (Eastman et al. 1995). A final map of flood risk was created for Amman Governorate

Fig. 7. Photographs of frequent flooding in Amman city: (a) 3 Nov 2014, (b) 5 Nov 2015, (c) 26 Oct 2018, (d) 28 Feb 2019, (e) 15 Dec 2020, (f) 4 Nov 2021

to show the spatial distribution of flood sites. In addition to developing the flood risk maps to notify the people responsible at all levels of decision-making and planners with the aim to providing sustainable soil and water conservation practices, reducing infrastructure damage, and financial and human losses, etc. (Fig. 5).

The areas with high and very high flood risk in Amman are about 19.8% and 8.4% of the total area, respectively. As for the areas with low and very low flood risk, they are about 27.2% and 14.5%, respectively, of the total area of the study area (Table 14).

In the end, it was found that the urban areas in the Greater Amman Municipality were affected by a very high risk of flooding, especially in the north-western regions with high population density, such as the areas of Ras al-Ain, Madinah, Qweismeh, Muqabalin, Sweileh, Jubaiha and Zahran. As for the areas in which the level of flood risk is classified as high, they include Naour, Al-Yadudah, Shafa Badran, Wadi Al-Seir, Abu Nuseir, Sahab and Al-Quweismeh. By contrast, the eastern, south-eastern, and western arid and semi-arid regions of Amman have low and very low flood probability, and they have low population density as well (Fig. 6).

Some photographs of flooding in Amman and its recurrence in recent years, and the resulting severely damaged public and private property and infrastructure, interruption of public life, financial

losses, etc. are shown in Figure 7. For additional detail, visit: (https://www.jordantimes.com/news/local/capital%E2%80%99s-topography-volume-rain-over-short-period-blamed-intensity-flash-floods).

Conclusions

The application of AHP integrated into Geographic Information Systems (GIS) is one of the most important methods for creating flood risk maps. As is well known, it is very important to assess and analyze flood risk areas in different regions of the world, especially where flooding is a dominant phenomenon that has economic, social and environmental effects. The numerous construction sites in the capital Amman were probably a major reason behind the flooding and the shrinking empty space in the city that would usually absorb rainfall. In addition to the damage to infrastructure, the largest damage was caused to shops and stores that were raided by floods. Moreover, climate change is related to the recurrence of atmospheric instability, and the accompanying large amounts of rain during short periods of time; thus, flooding could reach its peak within a shorter period of time. This requires the effective management of flood risk areas within the study area and the expansion of water harvesting projects in areas of high and very high levels of flood risk. Finally, the methodology used in this study can be considered a useful tool for predicting potential flood areas and thus avoiding flood damage and ensuring public safety.

Acknowledgement

Special thanks to the following agencies for their assistance with this research, namely, the United States Geological Survey (USGS), and the National Aeronautics and Space Administration (NASA) for providing Landsat-8 images free of cost. Also, we would like to thank the department of meteorology of Jordan, the ministry of agriculture, and the ministry of water and irrigation.

References

AHER P, ADINARAYANA J and GORANTIWAR S, 2013, Prioritization of watersheds using multi-criteria evaluation through the fuzzy analytical hierarchy process. *Agricultural Engineering International: CIGR Journal* 15(1): 11–18. https://cigrjournal.org/index.php/Ejounral/article/view/2282/1695.

AIKHUELE D, SOULEMAN F and AMIR A, 2014, Application of fuzzy AHP for ranking critical success factors for the successful implementation of Lean Production Technique. A*ustralian Journal of Basic and applied sciences* 8(18): 399-407.

AL-QUDAH K and ABU-JABER N, 2009, A GIS database for sustainable management of shallow water resources in the Tulul Ashaqif region, NE Jordan. *Water Resources Management Journal* 23: 603-615. DOI: 10.1007/s11269-008-9290-4.

AL RAISI S, SULAIMAN H, ABDALLAH O and SULIMAN F, 2014, Landfill suitable analysis using AHP method and state of heavy metals pollution in selected landfills in Oman. *European Scientific Journal* 10(17). DOI: 10.19044/esj.2014.v10n17p%25p.

AL-SABABHAH N, 2018, Assessment of Flood Vulnerability in Arid Basins from a Geomorphological Perspective (Wadi Musa in Southern Jordan: Case Study). *Journal of the Faculty of Arts (JFA)* 78(7): 267-296.

AL-SABABHAH N, 2022, Development of landslide susceptibility mapping using GIS modeling in Jordan's northern highlands. *Environment and Ecology Research* 10(6): 701-727. DOI: 10.13189/eer.2022.100607.

AL-SABABHAH N, 2023, Topographic Position Index to Landform Classification and Spatial Planning, Using GIS, for Wadi Araba, South West Jordan. *Environment and Ecology Research*, 11(1): 79-101. DOI: 10.13189/eer.2023.110106.

ANDUALEM T, HAGOS Y, KEFALE A, and ZELALEM B, 2020, Soil erosion-prone area identification using multi-criteria decision analysis in Ethiopian highlands. *Modeling Earth Systems and Environment* 6: 1407–1418. DOI: 10.1007/s40808-020-00757-2.

AYALEW L and YAMAGISHI H, 2005, The application of GIS-based logistic regression for landslide susceptibility mapping in the Kakuda–Yahiko Mountains, Central Japan. *Geomorphology* 65(2): 15–31. DOI: 10.1016/j.geomorph.2004.06.010.

BUNRUAMKAEW K and MURAYAMA Y, 2011, Site Suitability Evaluation for Ecotourism Using GIS & AHP: A Case Study of Surat Thani Province,

Thailand. *Procedia – Social and Behavioral Sciences* 21: 269-278. DOI: 10.1016/j.sbspro.2011.07.024.

CANADA J and GREEN K, 1999, *Assessing the Accuracy of Remotely sensed data: Principles and practices*. Lewis publishers, USA.

CHAUDHARY P, CHHETRI S, JOSHI K, SHRESTHA B and KAYASTHA P, 2016, Application of an Analytic Hierarchy Process (AHP in the GIS interface for suitable fire site selection: A case study from Kathmandu Metropolitan City, Nepal. *Socio-Economic Planning Services*: 60 –71. DOI: 10.1016/j.seps.2015.10.001.

CHEN C, 2006, Applying the analytical hierarchy process (AHP) approach to convention site selection. *Journal of Travel Research* 45(2): 167–174. DOI: 10.1177/0047287506291593.

DANIELSON T, 2013, Utilizing a high-resolution digital elevation model (DEM) to develop a stream power index (SPI) for the Gilmore creek watershed in Winona county, Minnesota. *Papers in Resource Analysis*, 15: 1-11.

EASTMAN J, WEIGEN J, KYEM P and TOLEDANO J, 1995, For storm prediction and flood forecasting. tech. report flooded project, (action 3.1) *Interreg IIB cases. research institute for geo-hydrological protection (IRPI-CNR)*, Italy. DOI: 10.1080/02626667.2011.555836.

FALKLAND A, 1993, Hydrology and water management on small tropical islands, Hydrology of Warm Humid Regions. *Proceedings of the Yokohama Symposium, IAHS Publ.* no. 216, Hydrology and Water Resources Branch, ACT Electricity and Water. Australia https://iahs.info/uploads/dms/iahs_216_0263.pdf.

GREENBAUM N, SCHWARTZ U and BERGMAN N, 2010, Extreme floods and short-term hydro climatological fluctuations in the hyper-arid Dead Sea region. *Global and Planter Change* 70(1-4): 125-137.

HAILE A and RIENTJES T, 2005, Effects of LiDAR DEM resolution in flood modeling: a model sensitivity study for the city of Tegucigalpa, Honduras. *ISPRS WG III/3, III/4, V/3 Workshop*, Netherlands, September 12-14, 2005.

HUTCHINSON M, 1998, Interpolation of rainfall data with thin plate smoothing splines - part II: analysis of topographic dependence. *Journal of Geographic information and Decision analysis* 2(2): 152 -167.

Intergovernmental Panel on Climate Change (IPCC (Report. The Fourth Assessment Report (AR4), 2008, Was prepared under the auSPIces of the IPCC, which is chaired by Dr. Rajendra K. Pachauri, and administered by the IPCC Working Group II Technical Support Unit. https://www.ipcc.ch/site/assets/uploads/2018/03/doc13-5.pdf.

JOUBERT A, LEIMAN A, DE KLERK H, KATU S and AGGENBACH J, 1997, Fynbos (fine bush) vegetation and the supply of water: a comparison of multi-criteria decision analysis. *Ecological Economics* 22(2): 123–140. DOI: 10.1016/S0921-8009(97)00573-9.

KAKEMBO V, XANGA W and ROWNTREE K, 2009, Topographic Thresholds in Gully Development On the Hillslopes of Communal Areas in Ngqushwa Local Municipality, Eastern Cape, South Africa. *Geomorphology* 110: 188–194. DOI: https://doi.org/10.1016/j.geomorph.2009.04.006.

KELLENS W, DECKERS P, SALEH H and VANNEUVILLE W, 2008, A GIS tool for flood risk analysis in Flanders (Belgium). *Risk Analysis* 39: 21–27. DOI: 10.2495/RISK080031.

KOURGIALAS N and KARATZAS G, 2011, Flood management and a GIS modelling method to assess flood-hazard areas: A case study. *Hydrological Sciences Journal* 56(2): 212–225. DOI: 10.1080/02626667.2011.555836.

MALCZEWSKI J, 1999, *GIS and Multi-Criteria Decision Analysis*. New York: John Wiley and Sons.

MALCZEWSKI J, 2006, GIS-Based Multicriteria Decision Analysis: A Survey of the Literature". *International Journal of Geographical Information Science* 20 (7): 703-726. DOI: 10.1080/13658810600661508.

MOORE I, RODGER B, GRAYSON, 1991, Terrain-based catchment partitioning and runoff prediction using vector elevation data. *Water Resources Research* 27(6): 1177–1191. DOI: 10.1029/91WR00090.

NAWAISEH S and AL-SABABHAH N, 2017, Synoptic conditions associated with Flash flood, which affected the city of Aqaba on 29 March 2015. *Humanities and Social Sciences Series* (Mutah University) 32(3): 175-202.

NEFESLIOGLU H, GOKCEOGLU C and SONMEZ H, 2008, An assessment on the use of logistic regression and artificial neural networks with different sampling strategies for the preparation of landslide susceptibility maps. *Engineering Geology* 97: 171–191. DOI: 10.1016/j.enggeo.2008.01.004.

NIE W, YUAN Y, KEPNER W, NASH M, JACKSON M and ERICKSON C, 2011, Assessing impacts of land use and land cover changes on hydrology for the upper San Pedro watershed. *Journal of Hydrology* 407(1–4): 105– 114.

OZKAN S and TARHAN C, 2016, Detection of Flood Hazard in Urban Areas Using GIS: Izmir Case. *Procedia Technology* 22: 373-381. DOI: 10.1016/j.protcy.2016.01.026.

POTTER K and FREVERT D , 2010, *Proceedings of watershed management 2010: innovations in watershed management under land use and*

climate change. Madison, 23-27 August 2010, American society of civil engineers. DOI: 10.1061/9780784411438.

PUNO G and AMPER R, 2016, Flood Modeling of Musimusi River in Balingasag. *Misamis Oriental* 20(3): 150-165.

RAN Q, SU D, LI P and HE Z, 2012, Experimental study of the impact of rainfall characteristics on runoff generation and soil erosion. *Journal of Hydrology*: 99–111. DOI: 10.1016/j.jhydrol.2011.12.035.

RIBEIRO R, 1996, Fuzzy multiple criterion decision making: a review and new preference elicitation techniques. *Fuzzy Sets and Systems* 78(2): 155-181. DOI: 10.1016/0165-0114(95)00166-2.

SAATY T, 1977, A scaling method for priorities in hierarchical structures. *Journal of Mathematical Psychology* 15: 234-281.

SAATY T, 1980, *The analytic hierarchy process*. McGraw-Hill: New York

SAATY T, 1984, The analytic hierarchy process: decision making in complex environments. In: Avenhaus R, Huber RK (eds). *Quantitative Assessment in Arms Control*. Plenum Press, New York. DOI: 10.1007/978-1-4613-2805-6_12.

SAATY T, 2008, Decision making with the analytic hierarchy process. *International Journal of Services Sciences* 1(1): 16.

SAATY R, 2016, Decision making in complex environments: the analytic network process (ANP) for dependence and feedback. Katz Graduate School of Business University of Pittsburg, vol. I.

SINSHAW B, BELETE A, TEFERA A, DESSIE A, BIZUNEH B, ALEM H, ATANAW S, ESHETE D, WUBETU T, ATINKUT H, and MOGES M, 2021, Prioritization of potential soil erosion susceptibility region using fuzzy logic and analytical hierarchy process, upper Blue Nile Basin, Ethiopia. *Water-Energy Nexus* 4: 10–24. DOI: 10.1016/j.wen.2021.01.001.

STEWART T and SCOTT L, 1995, A Scenario-Based Framework for Multi-criteria Decision Analysis in Water Resources Planning. *Water Resources Research* 31(11): 2835–2843. DOI: 10.1029/95WR01901.

TAIRI A, ELMOUDEN A and ABOULOUAFA M, 2013, Soil Erosion RiskMapping Using the Analytical Hierarchy Process (AHP) and GeographicInformation System in the Tifnout-Askaoun Watershed, Southern Morocco. *European Scientific Journal* 15(30): 338. DOI: 10.19044/esj.2019.v15n30p338.

United States Department of Agriculture (USDA), 2004, Hydrologic soil-cover complexes, natural resources conservation service, chapter 9, part 630 hydrology, national engineering handbook, USA.

YASSER M, JAHANGIR K and MOHMMAD A, 2013, Earth dam site selection using the analytic hierarchy process (AHP): A case study in the west of Iran. *Arabian Journal of Geoscience* 6(9): 3417–3426. DOI: 10.1007/s12517-012-0602-x.

ZERGER A, 2002, Examining GIS decision utility for natural hazard risk modeling. *Environmental Modelling and Software* 17(3): 287–294. DOI: 10.1016/S1364-8152(01)00071-8.

Received 11 August 2022
Accepted 17 April 2023